An NMPC design for stabilizing thrust-propelled underactuated vehicles

Ngoc Thinh Nguyen Ionela Prodan Laurent Lefèvre

Univ. Grenoble Alpes, Grenoble INP, LCIS, F-26000, Valence, France,
Email: {ngoc-thinh.nguyen,ionela.prodan,laurent.lefevre}@lcis.grenoble-inp.fr

4 June 2018

Outline

Motivation

Experimental setup with Crazyflie 2.0 quadcopter platform at LCIS

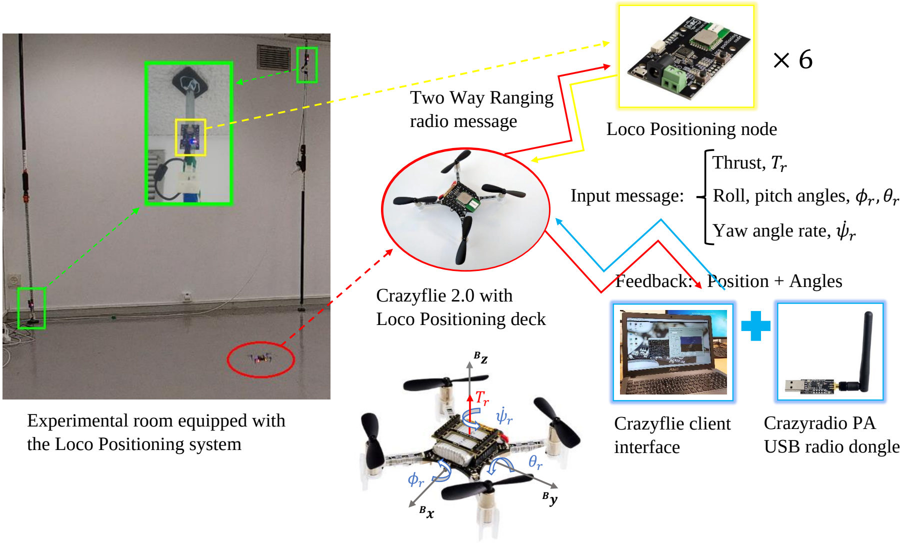

N.T. Nguyen, I. Prodan, L. Lefèvre: *Flat trajectory design and tracking with saturation guarantees: a nano-drone application*, submitted to International Journal of Control. Available upon request.

Motivation

Quadcopter trajectory tracking

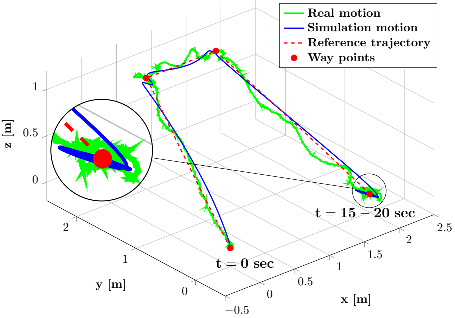

Experimental results using a feedback linearization control design.

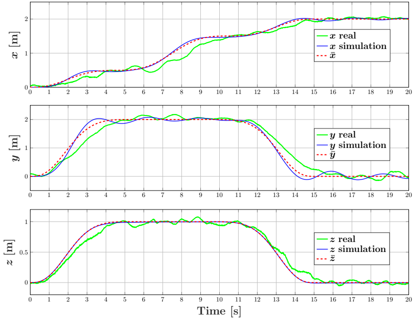

Tracking results of the three axes.

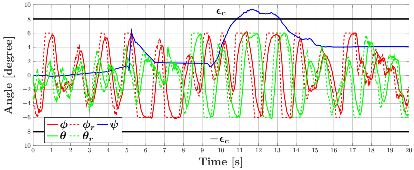

Tracking results of the three Euler angles.

Achievements:

- Good experimental platform for studying various control algorithms.
- Feedback linearization control successfully implemented with good tracking results.

N.T. Nguyen, I. Prodan, L. Lefèvre: *Flat trajectory design and tracking with saturation guarantees: a nano-drone application*, submitted to International Journal of Control. Available upon request.

Motivation

Quadcopter trajectory tracking

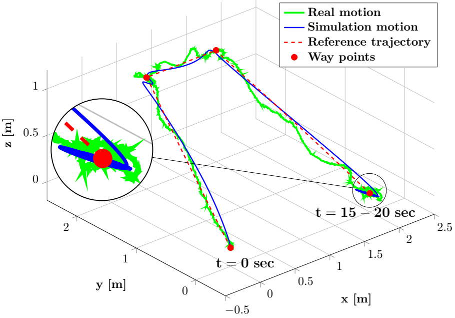

Experimental results using a feedback linearization control design.

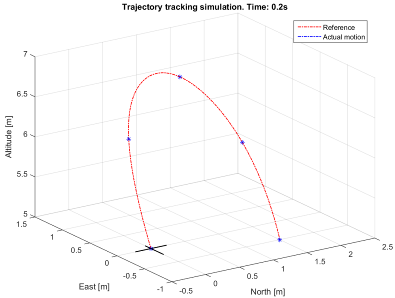

Simulation results using a hierarchical MPC control design.

Achievements:

- Good experimental platform for studying various control algorithms.
- Feedback linearization control successfully implemented with good tracking results.

Achievements:

- Two-layer MPC design combined with feedback linearization.
- Good tracking results with state and input constraints satisfactions.

N.T. Nguyen, I. Prodan, L. Lefèvre: *Multi-layer optimization-based control design for quadcopter trajectory tracking*, in Proc. of the 25th IEEE Mediterranean Conference on Control and Automation (MED'17), p.601-606,2017.

Motivation

Can we design an NMPC scheme with recursive feasibility and asymptotic stability?
If so, under what limitations and with what performances?

Open issues:

- Linearize the system's dynamics around the equilibrium point and design a linear MPC. Stability proofs are not considered [Zanelli, Horn, Frison, and Diehl (2018); Nguyen, Prodan, and Lefèvre (2017a); Zhao and Go (2014); Bemporad, Pascucci, and Rocchi (2009)].
- Consider the system's jerks as inputs of the NMPC design and decouple the motions along the three axes for constraints fulfillment on thrust and angular velocities. No stability guarantees are imposed [Singhal and Sujit (2015); Hehn and D'Andrea (2011)].
- Consider an NMPC design without terminal cost and terminal constraint. Only recursive feasibility guarantees are considered [Ribeiro, Conceição, Sa, and Corke (2015)].

Outline

Nonlinear Model Predictive Control

Rawlings and Muske (1993); Chen and Allgöwer (1998); Mayne et al. (2000); Mayne (2014)
Solve the open-loop optimal control problem at time t using the measured state $\boldsymbol{x}(t)$ and the prediction horizon T_p:

$$\min_{\bar{\boldsymbol{u}}(\cdot)} \int_t^{t+T_p} \ell(\bar{\boldsymbol{x}}(\tau,t), \bar{\boldsymbol{u}}(\tau,t))\, d\tau + F(\bar{\boldsymbol{x}}(T_p,t))$$

subject to:

$$\begin{cases} \dot{\bar{\boldsymbol{x}}} = f(\bar{\boldsymbol{x}}, \bar{\boldsymbol{u}}) \text{ (system dynamics)}, \\ \bar{\boldsymbol{x}}(\tau,t) \in \mathcal{X},\ \bar{\boldsymbol{u}}(\tau,t) \in \mathcal{U},\ \forall \tau \in [t, t+T_p] \text{ (state and input constraints)}, \\ \bar{\boldsymbol{x}}(t,t) = \boldsymbol{x}(t) \text{ (initial condition)}, \\ \bar{\boldsymbol{x}}(t+T_p,t) \in \mathcal{X}_f \text{ (terminal constraint set)}. \end{cases}$$

Apply to the system at time $\tau \in [t, t+\delta]$ the optimal control action:

$$\boldsymbol{u}_{\text{MPC}}(\tau,t) = \bar{\boldsymbol{u}}^*(\tau, \boldsymbol{x}(t)),\ \forall \tau \in [t, t+\delta],$$

with the sampling time $\delta < T_p$ chosen such that the state measurement is accomplished.

Assumptions:

- The control action has to stabilize the system around the equilibrium $\{\boldsymbol{x}_e, \boldsymbol{u}_e\}$.
- The stage cost $\ell : \mathcal{X} \times \mathcal{U} \to \mathbb{R}$ satisfies $\ell(\boldsymbol{x}, \boldsymbol{u}) > 0\ \forall (\boldsymbol{x}, \boldsymbol{u}) \in \mathcal{X} \times \mathcal{U} \backslash \{\boldsymbol{x}_e, \boldsymbol{u}_e\}$ and $\ell(\boldsymbol{x}_e, \boldsymbol{u}_e) = 0$.
- The terminal cost $F : \mathcal{X} \to \mathbb{R}$ satisfies $F(\boldsymbol{x}) > 0\ \forall \boldsymbol{x} \in \mathcal{X} \backslash \{\boldsymbol{x}_e\}$ and $F(\boldsymbol{x}_e) = 0$.

Stability conditions of NMPC design with invariant set

The recursive feasibility[3] and the asymptotic (exponential) stability of the closed-loop controlled system are guaranteed if the following conditions are satisfied (Mayne et al. (2000)):

(C1) [State constraints fulfillment] $\mathcal{X}_f \subseteq \mathcal{X}$, $\boldsymbol{x}_e \in \mathcal{X}_f$.

(C2) [Input constraints fulfillment] There exists a local controller $\boldsymbol{u}_{\text{loc}}(\boldsymbol{x})$ such that $\boldsymbol{u}_{\text{loc}}(\boldsymbol{x}) \in \mathcal{U}, \ \forall \boldsymbol{x} \in \mathcal{X}_f$.

(C3) [Positive invariant terminal set] $\mathcal{X}_f$ is positively invariant under $\boldsymbol{u}_{\text{loc}}(\boldsymbol{x})$.

(C4) [Local Lyapunov function existence] The stage and terminal costs $\ell(\boldsymbol{x}, \boldsymbol{u}), F(\boldsymbol{x})$ under $\boldsymbol{u}_{\text{loc}}(\boldsymbol{x})$ (i.e., $\dot{\boldsymbol{x}} = f(\boldsymbol{x}, \boldsymbol{u}_{\text{loc}}(\boldsymbol{x}))$) satisfy:

$$\frac{dF(\boldsymbol{x})}{dt} + \ell\left(\boldsymbol{x}, \boldsymbol{u}_{\text{loc}}(\boldsymbol{x})\right) \leq 0, \ \forall \boldsymbol{x} \in \mathcal{X}_f.$$

[3] feasibility obtained with the assumption of the first successfully executing iteration.

State-of-the-art on NMPC stability with terminal constraint

Various approaches are employed in the literature for stability guarantees:

• NMPC with terminal equality constraint (Keerthi and Gilbert (1988); Rawlings and Muske (1993))

$\mathcal{X}_f = \{\boldsymbol{x}_e\}$, $F(\boldsymbol{x}) \triangleq 0$ and $\boldsymbol{u}_{\text{loc}} = 0$.

• Quasi-infinite horizon NMPC (Chen and Allgöwer (1998))

$\mathcal{X}_f$ is an ellipsoidal invariant set under linear feedback controller.

• NMPC with polytopic invariant set (Cannon, Deshmukh, and Kouvaritakis (2003))

$\mathcal{X}_f$ is a polytopic invariant terminal set under linear feedback controller $\boldsymbol{u}_{\text{loc}}$, applied for input-affine nonliner system.

• NMPC design employing a feedback linearization law (Simon, Löfberg, and Glad (2013))

A feedback linearization law is applied to linearize the considered nonlinear system. Then, an NMPC controller is designed under the varying input constraint set.

• NMPC design with invariance induced by a computed-torque control law (Nguyen, Prodan, and Lefèvre (2018b))

$\mathcal{X}_f$ is an ellipsoidal invariant set under nonlinear computed-torque controller $\boldsymbol{u}_{\text{loc}}$.

Outline

Returning and bounding regions

Definition: Consider a general system $\dot{\boldsymbol{x}} = f(\boldsymbol{x}, \boldsymbol{u})$ admitting a feedback controller $\boldsymbol{u}_b(\boldsymbol{x})$ and two compact sets $\mathcal{R}_\delta$ and $\mathcal{B}_{\mathcal{R}_\delta}$ with $\mathcal{R}_\delta \subseteq \mathcal{B}_{\mathcal{R}_\delta}$ in the state-space dimension. Then, for a predefined $\delta > 0$, $\mathcal{R}_\delta$ is called *returning region* with time step δ and $\mathcal{B}_{\mathcal{R}_\delta}$ is called *bounding region* of $\mathcal{R}_\delta$ iff:

$$\boldsymbol{x}(t_0) \in \mathcal{R}_\delta \Rightarrow \begin{cases} \boldsymbol{x}(t_0+\delta) \in \mathcal{R}_\delta, \\ \boldsymbol{x}(t) \in \mathcal{B}_{\mathcal{R}_\delta},\ \forall t \in [t_0, t_0+\delta], \end{cases} \qquad \text{for any } t_0 \in \mathbb{R}.$$

Corollary:

- $\boldsymbol{x}(t_0) \in \mathcal{R}_\delta \Rightarrow \boldsymbol{x}(t) \in \mathcal{B}_{\mathcal{R}_\delta},\ \forall t \geq t_0.$
- Any positive invariant set is both a *returning region* (with any $\delta \geq 0$) and a *bounding region*. By considering these two distinct sets we generalize the control scheme and, arguably, increase its performance.

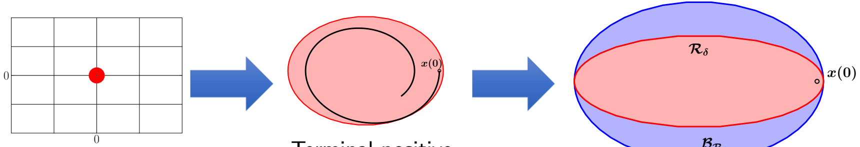

Terminal point | Terminal positive invariant set | *Returning* & *bounding* regions

NMPC stability conditions with returning and bounding regions

The recursive feasibility and the asymptotic stability of the system $\dot{\boldsymbol{x}} = f(\boldsymbol{x}, \boldsymbol{u})$ controlled by the NMPC controller are guaranteed if the following conditions are satisfied:

(C1*) [State and input constraints fulfillment] $\mathcal{B}_{\mathcal{R}_\delta} \subseteq \mathcal{X}$, $\boldsymbol{x}_e \in \mathcal{B}_{\mathcal{R}_\delta}$ and $\boldsymbol{u}_{\text{loc}}(\boldsymbol{x}) \in \mathcal{U}$, $\forall \boldsymbol{x} \in \mathcal{B}_{\mathcal{R}_\delta}$.

(C2*) [Returning region as terminal set] $\mathcal{R}_\delta$ serves as the terminal region $\mathcal{X}_f$ of the NMPC design.

(C3*) [Local Lyapunov function existence] Starting from any $\boldsymbol{x} \in \mathcal{R}_\delta$, the stage and terminal costs $\ell(\boldsymbol{x}, \boldsymbol{u})$, $F(\boldsymbol{x})$ under $\boldsymbol{u}_{\text{loc}}(\boldsymbol{x})$ (i.e., $\dot{\boldsymbol{x}} = f(\boldsymbol{x}, \boldsymbol{u}_{\text{loc}}(\boldsymbol{x}))$) satisfy:

$$\frac{dF(\boldsymbol{x})}{dt} + \ell\left(\boldsymbol{x}, \boldsymbol{u}_{\text{loc}}(\boldsymbol{x})\right) \leq 0.$$

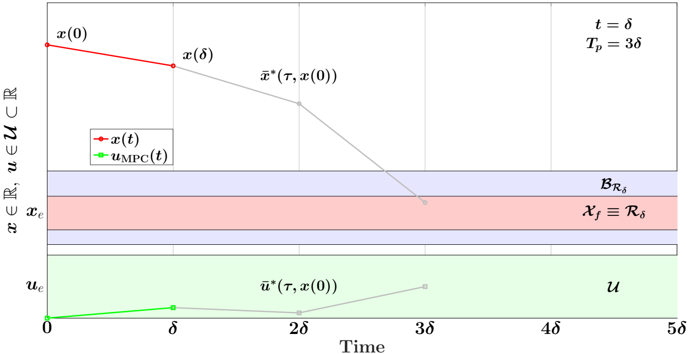

Outline

Thrust-propelled translation dynamics

Consider thrust-propelled translation dynamics (Mellinger and Kumar (2011); Nguyen et al. (2017b)):

$$\ddot{\xi} = \overrightarrow{g} + R\overrightarrow{T},$$

with $\xi \triangleq (x, y, z)^\top$ the position of the vehicle, $\overrightarrow{g} \triangleq (0, 0, -g)^\top$ the gravity, $\overrightarrow{T} \triangleq (0, 0, T)^\top$ the normalized thrust force and R the rotation matrix of the roll-pitch-yaw XYZ rotating sequence.

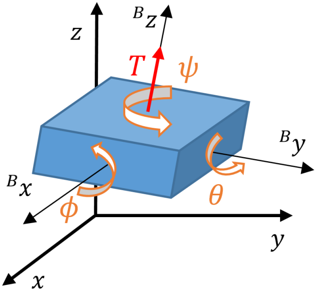

Thrust-propelled translation dynamics

Consider thrust-propelled translation dynamics (Mellinger and Kumar (2011); Nguyen et al. (2017b)):

$$\ddot{\xi} = \overrightarrow{g} + R\overrightarrow{T},$$

with $\xi \triangleq (x, y, z)^\top$ the position of the vehicle, $\overrightarrow{g} \triangleq (0, 0, -g)^\top$ the gravity, $\overrightarrow{T} \triangleq (0, 0, T)^\top$ the normalized thrust force and R the rotation matrix of the roll-pitch-yaw XYZ rotating sequence.

Its state-space representation is given by:

$$\dot{\boldsymbol{x}} = f(\boldsymbol{x}, \boldsymbol{u}) = A\boldsymbol{x} + h_\psi(\boldsymbol{u}),$$

with $A = \begin{bmatrix} 0_{3\times3} & \boldsymbol{I}_3 \\ 0_{3\times3} & 0_{3\times3} \end{bmatrix}$, $h_\psi(\boldsymbol{u}) = \begin{bmatrix} 0_{3\times1} \\ T(\cos\phi\sin\theta\cos\psi + \sin\phi\sin\psi) \\ T(\cos\phi\sin\theta\sin\psi - \sin\phi\cos\psi) \\ -g + T\cos\phi\cos\theta \end{bmatrix}$,

where $\boldsymbol{x} \triangleq (\xi^\top, \dot{\xi}^\top)^\top \in \mathbb{R}^6$ and $\boldsymbol{u} \triangleq (T, \phi, \theta)^\top \in \mathbb{R}^3$ (i.e., thrust, roll and pitch angles).

Specifications:

- The yaw angle ψ is an assumed known constant variable influencing the system.
- The equilibrium point is fixed at $\boldsymbol{x}_e = \boldsymbol{0}$ and $\boldsymbol{u}_e = [g\ 0\ 0]^\top$.
- The input $\boldsymbol{u}$ is constrained as: $\boldsymbol{u} \in \mathcal{U} = \{\boldsymbol{u} \in \mathbb{R}^3 |\ 0 \le T \le T_{limit}, |\phi| \le \epsilon_c, |\theta| \le \epsilon_c\}$, with $T_{limit} > g$ the thrust limit and $\epsilon_c \in (0, \pi/2)$ the desired maximum value of the angles.

Feedback linearization law

Mellinger and Kumar (2011); Formentin and Lovera (2011); Nguyen et al. (2017b)

Consider the feedback linearization law $\boldsymbol{u}_b(u, \psi) : \mathbb{R}^3 \times \mathbb{R} \to \mathbb{R}^3$ with $\boldsymbol{u}_b \triangleq [T_b\ \phi_b\ \theta_b]^\top$ and the virtual input vector $u \triangleq [u_x\ u_y\ u_z]^\top$:

$$T_b = \sqrt{u_x^2 + u_y^2 + (u_z + g)^2},$$
$$\phi_b = \arcsin\left(\frac{u_x \sin\psi - u_y \cos\psi}{\sqrt{u_x^2 + u_y^2 + (u_z + g)^2}}\right),$$
$$\theta_b = \arctan\left(\frac{u_x \cos\psi + u_y \sin\psi}{u_z + g}\right).$$

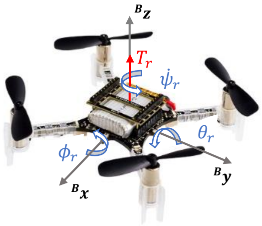

If $\boldsymbol{u}_b \in \mathcal{U}$, $\boldsymbol{u}_b$ linearizes the nonlinear system $\dot{\boldsymbol{x}} = A\boldsymbol{x} + h_\psi(\boldsymbol{u})$ into the linear stabilizable system:

$$\dot{\boldsymbol{x}} = A\boldsymbol{x} + h_\psi(\boldsymbol{u}_b(u, \psi)) \Leftrightarrow \dot{\boldsymbol{x}} = A\boldsymbol{x} + Bu \Leftrightarrow \begin{cases} \dot{x} = v_x, & \dot{v}_x = u_x, \\ \dot{y} = v_y, & \dot{v}_y = u_y, \\ \dot{z} = v_z, & \dot{v}_z = u_z, \end{cases}$$

with $B = [0_{3\times3}\ \boldsymbol{I}_3]^\top$.

Input constraint satisfaction with feedback linearization control

Input constraints:

$$\boldsymbol{u} \in \mathcal{U} = \{\boldsymbol{u} \in \mathbb{R}^3 |\ 0 \leq T \leq T_{limit}, |\phi| \leq \epsilon_c, |\theta| \leq \epsilon_c\},\ \ T_{limit} < g,\ \ \epsilon_c \in (0, \pi/2).$$

Lemma 1: [Bounds on virtual inputs]

By choosing three positive constants U_x, U_y and U_z such that:

$$U_z < g, \quad U_x^2 + U_y^2 \leq (-U_z + g)^2 \tan^2 \epsilon_c, \quad \sqrt{U_x^2 + U_y^2 + (U_z + g)^2} \leq T_{limit},$$

we have that, if $|u_x| \leq U_x$, $|u_y| \leq U_y$ and $|u_z| \leq U_z$, then $\boldsymbol{u}_b(u, \psi) \in \mathcal{U}$, $\forall \psi \in [-\pi, \pi]$.

Proof sketch: $|u_x| \leq U_x,\ |u_y| \leq U_y,\ |u_z| \leq U_z$ imply that:

$$T_b \leq \sqrt{U_x^2 + U_y^2 + (U_z + g)^2},$$

$$|\phi_b|, |\theta_b| \leq \arctan\left(\sqrt{\frac{U_x^2 + U_y^2}{(-U_z + g)^2}}\right).$$

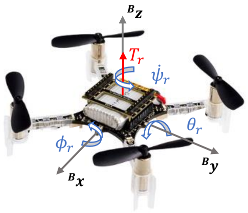

N.T. Nguyen, I. Prodan, L. Lefèvre: *Flat trajectory design and tracking with saturation guarantees: a nano-drone application*, submitted to International Journal of Control. Available upon request.

Returning and bounding regions with input constraint satisfaction

Lemma 2: [Returning and bounding regions formulation]

Consider the sampling time δ of the NMPC controller, then, define three pole vector as follows:

$$s_q \triangleq [s_{1_q} \ s_{2_q}]^\top \in \mathcal{S}_\delta, \ q \in \{x, y, z\},$$

with the set $\mathcal{S}_\delta =$

$$\left\{ s = \begin{bmatrix} s_1 \\ s_2 \end{bmatrix} \middle| \begin{cases} s_1 < s_2 < 0 \ (\text{closed-loop stability}) \\ \dfrac{\lambda_2(s,\delta)}{1-\lambda_1(s,\delta)} \leq \dfrac{1-|\lambda_4(s,\delta)|}{-\lambda_3(s,\delta)} \ (\text{existence of returning and bounding regions}) \end{cases} \right\},$$

$$\lambda_1(s,t) = \frac{s_2 e^{s_1 t} - s_1 e^{s_2 t}}{s_2 - s_1}, \qquad \lambda_2(s,t) = \frac{e^{s_2 t} - e^{s_1 t}}{s_2 - s_1},$$

$$\lambda_3(s,t) = \frac{s_1 s_2 (e^{s_1 t} - e^{s_2 t})}{s_2 - s_1}, \qquad \lambda_4(s,t) = \frac{s_2 e^{s_2 t} - s_1 e^{s_1 t}}{s_2 - s_1}.$$

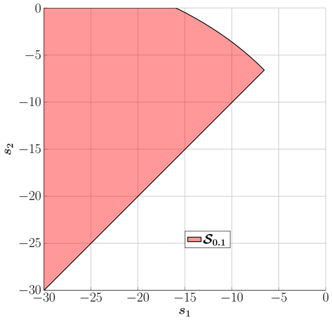

Illustration of S_δ with $\delta = 0.1$ seconds.

Returning and bounding regions with input constraint satisfaction

Lemma 2: [Returning and bounding regions formulation]

Consider the sampling time δ of the NMPC controller, then, define three pole vector as follows:

$$s_q \triangleq [s_{1_q} \;\; s_{2_q}]^\top \in \mathcal{S}_\delta, \;\; q \in \{x, y, z\},$$

which ensure the existence of the returning and bounding regions.

This allows to define three pairs of $X_q > 0$ and $V_q > 0$ such that:

$$\frac{\lambda_2(s_q, \delta)}{1 - \lambda_1(s_q, \delta)} \leq \frac{X_q}{V_q} \leq \frac{1 - |\lambda_4(s_q, \delta)|}{-\lambda_3(s_q, \delta)},$$

$$K_{p_q} \widetilde{X}_q + K_{d_q} \widetilde{V}_q \leq U_q, \text{with } K_{p_q} = s_{1_q} s_{2_q}, \;\; K_{d_q} = -s_{1_q} - s_{2_q},$$

which describe the size of the returning and bounding regions.

$$\widetilde{X}_q \triangleq \widetilde{X}(X_q, V_q, s_q, \delta) = \max_{t \in [0, \delta]} \{X_q \lambda_1(s_q, t) + V_q \lambda_2(s_q, t)\},$$

$$\widetilde{V}_q \triangleq \widetilde{V}(X_q, V_q, s_q, \delta) = \max_{t \in [0, \delta]} \{-X_q \lambda_3(s_q, t) + V_q |\lambda_4(s_q, t)|\}.$$

Returning and bounding regions with input constraint satisfaction

Lemma 2: [Returning and bounding regions formulation]

Consider the sampling time δ of the NMPC controller, then, define three pole vector as follows:

$$s_q \triangleq [s_{1_q}\ \ s_{2_q}]^\top \in \mathcal{S}_\delta,\ \ q \in \{x, y, z\},$$

which ensure the existence of the returning and bounding regions.

This allows to define three pairs of $X_q > 0$ and $V_q > 0$ such that:

$$\frac{\lambda_2(s_q, \delta)}{1-\lambda_1(s_q,\delta)} \le \frac{X_q}{V_q} \le \frac{1-|\lambda_4(s_q,\delta)|}{-\lambda_3(s_q,\delta)},$$
$$K_{p_q}\widetilde{X}_q + K_{d_q}\widetilde{V}_q \le U_q, \text{with } K_{p_q} = s_{1_q}s_{2_q},\ \ K_{d_q} = -s_{1_q} - s_{2_q},$$

which describe the size of the returning and bounding regions.

Then, consider two sets $\mathcal{R}_\delta$ and $\mathcal{B}_{\mathcal{R}_\delta}$ defined as follows:

$$\mathcal{R}_\delta = \left\{ \boldsymbol{x} \in \mathbb{R}^6 \,\middle|\, \begin{cases} |x| \le X_x,\ |v_x| \le V_x \\ |y| \le X_y,\ |v_y| \le V_y \\ |z| \le X_z,\ |v_z| \le V_z \end{cases} \right\}, \quad \mathcal{B}_{\mathcal{R}_\delta} = \left\{ \boldsymbol{x} \in \mathbb{R}^6 \,\middle|\, \begin{cases} |x| \le \widetilde{X}_x,\ |v_x| \le \widetilde{V}_x \\ |y| \le \widetilde{X}_y,\ |v_y| \le \widetilde{V}_y \\ |z| \le \widetilde{X}_z,\ |v_z| \le \widetilde{V}_z \end{cases} \right\},$$

for any constant value of $\psi \in [-\pi, \pi]$, we have that:

1) $\boldsymbol{u}_b(K\boldsymbol{x}, \psi) \in \mathcal{U},\ \forall \boldsymbol{x} \in \mathcal{B}_{\mathcal{R}_\delta}$ with $K = -\left[\mathrm{diag}(K_{p_x}, K_{p_y}, K_{p_z})\ \ \mathrm{diag}(K_{d_x}, K_{d_y}, K_{d_z})\right]$;
2) $\mathcal{R}_\delta$ and $\mathcal{B}_{\mathcal{R}_\delta}$ are the *returning* and *bounding* regions with time step δ under $\boldsymbol{u}_b(K\boldsymbol{x}, \psi)$.

Proof of Lemma 2 [Returning & bounding regions formulation]

For all $\boldsymbol{x} \in \mathcal{B}_{\mathcal{R}_\delta}$, $u = K\boldsymbol{x}$, with $K = -\left[\mathrm{diag}(K_{p_x}, K_{p_y}, K_{p_z}) \;\; \mathrm{diag}(K_{d_x}, K_{d_y}, K_{d_z})\right]$ leads to:

- $u_q = K_{p_q} q + K_{d_q} v_q \Rightarrow |u_q| \leq K_{p_q}|q| + K_{d_q}|v_q| \leq K_{p_q}\widetilde{X}_q + K_{d_q}\widetilde{V}_q \leq U_q,\;\; q \in \{x, y, z\}$.
- $\boldsymbol{u}_b(K\boldsymbol{x}, \psi) \in \mathcal{U}, \forall \psi \in [-\pi, \pi]$ by Lemma 1 [Bounds on virtual inputs].
- $\boldsymbol{u}_b(K\boldsymbol{x}, \psi)$ linearizes the nonlinear system into:

$$\dot{\boldsymbol{x}} = A\boldsymbol{x} + h_\psi(\boldsymbol{u}_b(K\boldsymbol{x}, \psi)) \Leftrightarrow \dot{\boldsymbol{x}} = A_K\boldsymbol{x} \Leftrightarrow \begin{cases} \dot{x} = v_x, & \dot{v}_x = -K_{p_x}x - K_{d_x}v_x, \\ \dot{y} = v_y, & \dot{v}_y = -K_{p_y}y - K_{d_y}v_y, \\ \dot{z} = v_z, & \dot{v}_z = -K_{p_z}z - K_{d_z}v_z. \end{cases}$$

Thus, $\mathcal{R}_\delta$ and $\mathcal{B}_{\mathcal{R}_\delta}$ are the *returning* and *bounding* regions with time step δ.

Illustrative example:

$T_{limit} = 2g$, $\epsilon_c = 10^\circ$.
$U_x = U_y = U_z = 1.0875$.
$s_x = s_y = s_z = [-16 \;\; -0.5]^\top$.
$X_x = X_y = X_z = 0.066$.
$V_x = V_y = V_z = 0.033$.
$\widetilde{X}_x = \widetilde{X}_y = \widetilde{X}_z = 0.0666$.
$\widetilde{V}_x = \widetilde{V}_y = \widetilde{V}_z = 0.033$.

$$\boldsymbol{x}_0 = \begin{bmatrix} X & -\frac{X}{2} & \frac{X}{2} & V & -V & V \end{bmatrix}^\top.$$

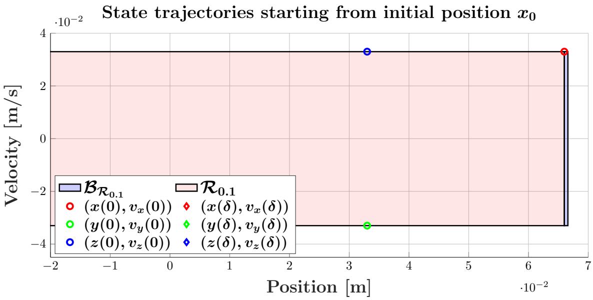

Stability conditions of NMPC design

Consider returning, $\mathcal{R}_\delta$ and bounding, $\mathcal{B}_{\mathcal{R}_\delta}$ regions with time step δ under $\boldsymbol{u}_{\text{loc}}(\boldsymbol{x})$:

(C1*) [State and input constraints fulfillment] $\mathcal{B}_{\mathcal{R}_\delta} \subseteq \mathcal{X}$, $\boldsymbol{x}_e \in \mathcal{B}_{\mathcal{R}_\delta}$ and $\boldsymbol{u}_{\text{loc}}(\boldsymbol{x}) \in \mathcal{U}$, $\forall \boldsymbol{x} \in \mathcal{B}_{\mathcal{R}_\delta}$.

(C2*) [Returning region as terminal set] $\mathcal{R}_\delta$ serves as the terminal region $\mathcal{X}_f$ of the NMPC design.

(C3*) [Local Lyapunov function existence] Starting from any $\boldsymbol{x} \in \mathcal{R}_\delta$, the stage and terminal costs $\ell(\boldsymbol{x}, \boldsymbol{u}), F(\boldsymbol{x})$ under $\boldsymbol{u}_{\text{loc}}(\boldsymbol{x})$ (i.e., $\dot{\boldsymbol{x}} = f(\boldsymbol{x}, \boldsymbol{u}_{\text{loc}}(\boldsymbol{x}))$) satisfy:

$$\frac{dF(\boldsymbol{x})}{dt} + \ell\left(\boldsymbol{x}, \boldsymbol{u}_{\text{loc}}(\boldsymbol{x})\right) \leq 0.$$

Proof steps:

For the thrust-propelled translation dynamics (ψ is a known constant), we have that:

- Conditions (C1*) and (C2*) are satisfied by Lemma 2 [Returning and bounding regions formulation]:
  - Consider $\boldsymbol{u}_{\text{loc}}(\boldsymbol{x}) \triangleq \boldsymbol{u}_b(K\boldsymbol{x}, \psi)$, with the corresponding $\mathcal{R}_\delta$ and $\mathcal{B}_{\mathcal{R}_\delta}$.
- For solving condition (C3*) :
  - $\ell(\boldsymbol{x}, \boldsymbol{u})$ is chosen such that $\ell\left(\boldsymbol{x}, \boldsymbol{u}_b(K\boldsymbol{x}, \psi)\right) \leq \boldsymbol{x}^\top Q^* \boldsymbol{x}, \forall \boldsymbol{x} \in \mathcal{B}_{\mathcal{R}_\delta}, \forall \psi \in [-\pi, \pi]$.
  - $F(\boldsymbol{x}) \triangleq \boldsymbol{x}^\top P \boldsymbol{x}$ where P is an unique positive definite symmetric matrix solution of:

$$A_K^\top P + P A_K + Q^* = 0.$$

$$\Rightarrow \frac{dF(\boldsymbol{x})}{dt} + \ell\left(\boldsymbol{x}, \boldsymbol{u}_{\text{loc}}(\boldsymbol{x})\right) \leq \boldsymbol{x}^\top (A_K^\top P + P A_K)\boldsymbol{x} + \boldsymbol{x}^\top Q^* \boldsymbol{x} = 0.$$

Stage cost and the upper bound for solving condition (C3*)

By considering $\boldsymbol{x}_e = \mathbf{0}$ and $\boldsymbol{u}_e = [g\ 0\ 0]^\top$, the stage cost is given as:

$$\ell(\boldsymbol{x}, \boldsymbol{u}) = \boldsymbol{x}^\top Q \boldsymbol{x} + r_T (T - g)^2 + r_\phi \tan^2 \phi + r_\theta \tan^2 \theta,$$

where $Q \in \mathbb{R}^{6\times 6}$ is positive definite and r_T, r_ϕ, r_θ are all positive scalars.

Lemma 3: [Bounds on the stage cost]

For all $\boldsymbol{x} \in \mathcal{B}_{\mathcal{R}_\delta}$, the stage cost $\ell(\boldsymbol{x}, \boldsymbol{u}_b(K\boldsymbol{x}, \psi))$ is bounded as follows:

$$\ell(\boldsymbol{x}, \boldsymbol{u}_b(K\boldsymbol{x}, \psi)) \leq \boldsymbol{x}^\top Q^* \boldsymbol{x},\ \forall \psi \in [-\pi, \pi],$$

where the positive definite matrix $Q^* \in \mathbb{R}^{6\times 6}$ is given as:

$$Q^* = Q + 3 r_T K^\top K + (r_\phi + r_\theta)\Gamma,$$

with the weighting matrix $\Gamma \in \mathbb{R}^{6\times 6}$, $\Gamma = \dfrac{1}{(-U_z + g)^2} K_{xy}^\top K_{xy}$, with $K_{xy} = \left[\mathrm{diag}(K_{p_x}, K_{p_y}, 0)\ \ \mathrm{diag}(K_{d_x}, K_{d_y}, 0)\right]$.

Proof sketch of Lemma 3 [Bounds on the stage cost]

- With $|u_z| \leq U_z < g$, the feedback linearization law $\boldsymbol{u}_b(u, \psi)$ is bounded as follows:

$$(T_b(u) - g)^2 = \left(\sqrt{u_x^2 + u_y^2 + (u_z + g)^2} - g\right)^2 \leq 3(u_x^2 + u_y^2 + u_z^2),$$

$$\tan^2(\phi_b(u, \psi)) \leq \frac{u_x^2 + u_y^2}{(-U_z + g)^2}, \ \forall \psi \in [-\pi, \pi], \text{ and similar result for } \theta_b(u, \psi).$$

- Employing $u = K\boldsymbol{x}$ (i.e., $u_q = K_{p_q} q + K_{d_q} v_q$, $\forall q \in \{x, y, z\}$), then, transform the results into quadratic formulations. $\square$

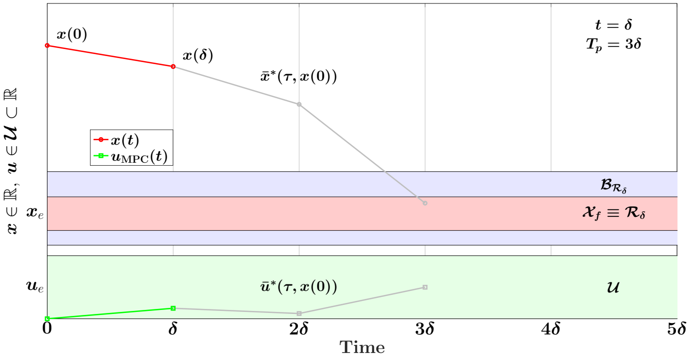

Summary of the NMPC design procedure

Step 1) Using Lemma 1, choose the saturation limits U_x, U_y and U_z in order to obtain the bounds on the virtual inputs of the feedback linearization law.

Step 2) Using Lemma 2, choose s_x, s_y and s_z within the set S_δ. Then, find three pairs X_q, V_q with $q \in \{x, y, z\}$ to obtain the *returning* region $\mathcal{R}_\delta$ which is then employed as the terminal region $\mathcal{X}_f$, hence, satisfying conditions (C1*) and (C2*).

Step 3) Choose the positive definite matrices $Q \in \mathbb{R}^{6\times 6}$ and three positive scalars r_T, r_ϕ, r_θ in order to obtain the stage cost $\ell(\boldsymbol{x}, \boldsymbol{u})$.

Step 4) Choose the prediction horizon T_p based on the computational constraint of the platform (e.g., the processing speed requirement).

Step 5) Using Lemma 3, define the matrix Q^*, then, solve the Lyapunov function for P in order to obtain the terminal cost $F(\boldsymbol{x})$ satisfying condition (C3*).

Outline

Simulation scenarios and tuning parameters

Crazyflie 2.0 nano-quadcopter: thrust limit $T_{limit} = 2g$ and maximum angle values $\epsilon_c = 10^\circ$.

Fixing the NMPC sampling time $\delta = 0.1$ seconds, two scenarios are considered as follows:

Scenario 1: Stabilizing the thrust-propelled translation dynamics with $\psi = 0$ using the proposed NMPC controller.

Table: Parameters of the proposed NMPC controller.

	Values
$U_x = U_y = U_z$	1.0875, 1.0875, 1.0875
$s_x = s_y = s_z$	$\begin{bmatrix} -16 & -0.5 \end{bmatrix}^\top$
$X_x = X_y = X_z$	0.066
$V_x = V_y = V_z$	0.033
Q	$10\boldsymbol{I}_6$
$r_T = r_\phi = r_\theta$	1
T_p	1 second
Q^*	$\begin{bmatrix} \mathrm{diag}\{204, 204, 202\} & \mathrm{diag}\{399, 399, 396\} \\ \mathrm{diag}\{399, 399, 396\} & \mathrm{diag}\{834, 834, 827\} \end{bmatrix}$
P	$\begin{bmatrix} \mathrm{diag}\{16.73, 16.73, 16.68\} & \mathrm{diag}\{12.73, 12.73, 12.63\} \\ \mathrm{diag}\{12.73, 12.73, 12.63\} & \mathrm{diag}\{25.77, 25.77, 25.55\} \end{bmatrix}$

Simulation scenarios and tuning parameters

Crazyflie 2.0 nano-quadcopter: thrust limit $T_{limit} = 2g$ and maximum angle values $\epsilon_c = 10^\circ$.

Fixing the NMPC sampling time $\delta = 0.1$ seconds, two scenarios are considered as follows:

Scenario 1: Stabilizing the thrust-propelled translation dynamics with $\psi = 0$ using the proposed NMPC controller.

Scenario 2: Stabilizing thrust-propelled translation dynamics with $\psi = 0$ using the quasi-infinite horizon NMPC controller (Chen and Allgöwer (1998)) with the ellipsoidal terminal region $\Omega_\alpha = \{\boldsymbol{x} \in \mathbb{R}^6 |\ \boldsymbol{x}^\top P_{qM} \boldsymbol{x} \leq \alpha\}$.

Table: Parameters of the quasi-infinite horizon NMPC controller.

	Values
Q_{qM}	$10\boldsymbol{I}_6$
R_{qM}	$\boldsymbol{I}_3$
T_p	1 second
K_{qM}	$\begin{bmatrix} 0 & 0 & -4 & 0 & 0 & -4 \\ 0 & 4/g & 0 & 0 & 4/g & 0 \\ -4/g & 0 & 0 & -4/g & 0 & 0 \end{bmatrix}$
κ	1
P_{qM}	$\begin{bmatrix} \text{diag}\{65.08, 65.08, 73\} & \text{diag}\{17.54, 17.54, 21.5\} \\ \text{diag}\{17.54, 17.54, 21.5\} & \text{diag}\{7.55, 7.55, 11.5\} \end{bmatrix}$
α	0.0035 (largest possible)

Simulation results with NMPC sampling time $\delta = 0.1$ seconds

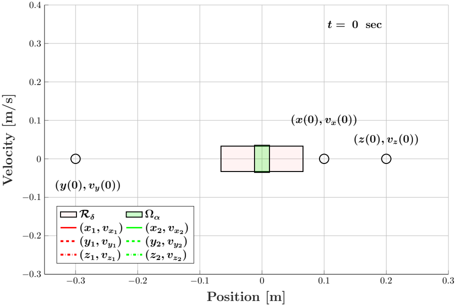

Terminal regions $\mathcal{R}_\delta$ and Ω_α (approximated illustration) and trajectories (x, v_x), (y, v_y), (z, v_z) under two scenarios.

Table: Comparisons between two scenarios.

	Scenario 1	Scenario 2
Volume $\mathcal{X}_f$	$> 13,600\%$	100%
Convergence time (seconds)	3	2.5
Computing time (seconds)	< 0.1	> 0.25

Yalmip (Löfberg (2004)), IPOPT (Wächter and Biegler (2006)), Matlab R2015a, Intel(R) Core(TM) i7-4720HQ CPU @2.60 GHz.

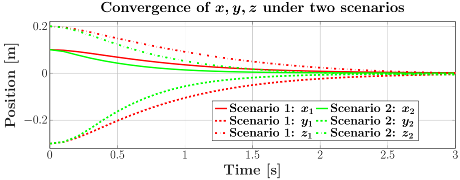

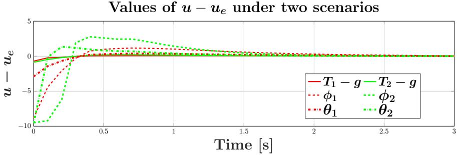

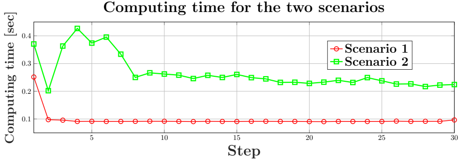

Outline

Conclusions and future developments

Conclusions:

- Characterization of returning and bounding regions with a specific time step.
- NMPC design guaranteeing recursive feasibility and asymptotic stability by employing the returning and bounding regions.
- NMPC design for stabilizing the thrust-propelled translation dynamics by using the nonlinear feedback lineariziation law as the local controller.
- Extensive simulations and comparisons with quasi-infinite horizon NMPC controller.

Future developments:

- Real implementation of the proposed NMPC controller on the Crazyflie 2.0 nano-quadcopter platform.
- NMPC design for stabilizing the class of systems possessing a computed-torque control law employing the returning and bounding regions (see also Nguyen et al. (2018b)).
- NMPC design guaranteeing recursive feasibility and stability with an attractive terminal region.

References

Alberto Bemporad, Carlo A Pascucci, and Claudio Rocchi. Hierarchical and hybrid model predictive control of quadcopter air vehicles. *IFAC Proceedings Volumes*, 42(17):14–19, 2009.

Mark Cannon, Venkatesh Deshmukh, and Basil Kouvaritakis. Nonlinear model predictive control with polytopic invariant sets. *Automatica*, 39(8): 1487–1494, 2003.

Hong Chen and Frank Allgöwer. A quasi-infinite horizon nonlinear model predictive control scheme with guaranteed stability. *Automatica*, 34(10): 1205–1217, 1998.

Simone Formentin and Marco Lovera. Flatness-based control of a quadrotor helicopter via feedforward linearization. In *Proceedings of the IEEE 50th Conference on Decision and Control (CDC-ECE'50)*, pages 6171–6176, 2011.

Markus Hehn and Raffaello D'Andrea. Quadrocopter trajectory generation and control. *IFAC Proceedings Volumes*, 44(1):1485–1491, 2011.

SS a Keerthi and Elmer G Gilbert. Optimal infinite-horizon feedback laws for a general class of constrained discrete-time systems: Stability and moving-horizon approximations. *Journal of optimization theory and applications*, 57(2):265–293, 1988.

J. Löfberg. Yalmip : A toolbox for modeling and optimization in MATLAB. In *Proceedings of the CACSD Conference*, Taipei, Taiwan, 2004. URL `http://users.isy.liu.se/johanl/yalmip`.

David Q Mayne. Model predictive control: Recent developments and future promise. *Automatica*, 50(12):2967–2986, 2014.

David Q Mayne, James B Rawlings, Christopher V Rao, and Pierre OM Scokaert. Constrained model predictive control: Stability and optimality. *Automatica*, 36(6):789–814, 2000.

Daniel Mellinger and Vijay Kumar. Minimum snap trajectory generation and control for quadrotors. In *IEEE International Conference on Robotics and Automation (ICRA)*, pages 2520–2525. IEEE, 2011.

Ngoc Thinh Nguyen, Ionela Prodan, and Laurent Lefèvre. Multi-layer optimization-based control design for quadcopter trajectory tracking. In *Proceedings of the 25th IEEE Mediterranean Conference on Control and Automation (MED'17)*, pages 601–606, 2017a.

Ngoc Thinh Nguyen, Ionela Prodan, Florin Stoican, and Laurent Lefèvre. Reliable nonlinear control for quadcopter trajectory tracking through differential flatness. *IFAC-PapersOnLine*, 50(1):6971–6976, 2017b. ISSN 2405-8963.

Ngoc Thinh Nguyen, Ionela Prodan, and Laurent Lefèvre. Effective angular constrained trajectory generation for thrust-propelled vehicles. *Accepted for publication at the 17th European Control Conference (ECC'18)*, 2018a.

Ngoc Thinh Nguyen, Ionela Prodan, and Laurent Lefèvre. NMPC design with invariance induced by a computed-torque control law. *Submitted to the 6th IFAC Conference on Nonlinear Model Predictive Control (NMPC'18), August, 2018. Available upon request*, 2018b.

Ngoc Thinh Nguyen, Ionela Prodan, and Laurent Lefèvre. Flat trajectory design and tracking with saturation guarantees: a nano-drone application. *Submitted to International Journal of Control. Available upon request*, Unpublished.

James B Rawlings and Kenneth R Muske. The stability of constrained receding horizon control. *IEEE Transactions on Automatic Control*, 38(10): 1512–1516, 1993.

Tiago T Ribeiro, André GS Conceição, Inkyu Sa, and Peter Corke. Nonlinear model predictive formation control for quadcopters. *IFAC-PapersOnLine*, 48 (19):39–44, 2015.

Daniel Simon, Johan Löfberg, and Torkel Glad. Nonlinear model predictive control using feedback linearization and local inner convex constraint approximations. In *2013 European Control Conference (ECC)*, pages 2056–2061. IEEE, 2013.

Rahul Singhal and PB Sujit. 3d trajectory tracking for a quadcopter using mpc on a 3d terrain. In *International Conference on Unmanned Aircraft Systems (ICUAS)*, pages 1385–1390. IEEE, 2015.

Andreas Wächter and Lorenz T Biegler. On the implementation of an interior-point filter line-search algorithm for large-scale nonlinear programming. *Mathematical programming*, 106(1):25–57, 2006.

Andrea Zanelli, Greg Horn, Gianluca Frison, and Moritz Diehl. Nonlinear model predictive control of a human-sized quadrotor. *Accepted for publication at the 17th European Control Conference (ECC'18)*, 2018.